Chinese Chemical Letters 37 (2026) 110655

Contents lists available at ScienceDirect

Chinese Chemical Letters

journal homepage: www.elsevier.com/locate/cclet

Electric tweezer for single microscopic particle trapping

Hui Li[a], Zhenjie Zhao[b], Bingqiang Ji[c], Jun Ma[a], Xuwu Zhang[d], Jingzhao Chen[a], Zhangran Ye[a], Zuankai Wang[e], Liqiang Zhang[a,*], Jianyu Huang[a,*], Yingdan Liu[b,*]

[a] Clean Nano Energy Center, State Key Lab of Metastable Materials Science and Technology, and College of Materials Science and Engineering, Yanshan University, Qinhuangdao 066004, China
[b] Center for Advanced Structural Materials, State Key Lab of Metastable Materials Science and Technology, and College of Materials Science and Engineering, Yanshan University, Qinhuangdao 066004, China
[c] School of Astronautics, Beihang University, Beijing 100191, China
[d] Nano-biotechnology Key Lab of Hebei Province, Yanshan University, Qinhuangdao 066004, China
[e] Department of Mechanical Engineering, The Hong Kong Polytechnic University, Hong Kong 999077, China

ARTICLE INFO

Article history:
Received 21 September 2024
Revised 7 November 2024
Accepted 19 November 2024
Available online 26 November 2024

Keywords:
Electric tweezers
Single particle trapping
Precisely manipulation
In-situ TEM
Microdevices assembly

ABSTRACT

Trapping and manipulating microscopic particles (micron or nano) in a liquid environment are of great significance for research and applications in nanoscience, engineering, and biomedicine. Although optical tweezers, magnetic tweezers, acoustic tweezers, *etc.* have been successfully developed, it is still challenging to separate, select, and manipulate micron and submicron particles with comparable morphologies and sizes in trace amounts of liquids with high viscosity and extremely tiny concentrations. Herein, an electric tweezer with measurable force was introduced in an environmental transmission electron microscope (ETEM) for trapping a single submicron particle in high viscosity liquids. The critical voltages for trapping SiO_2 and TiO_2 spheres were determined to be 75 V and 25 V, respectively, due to their dielectric characteristics. As a result, although TiO_2 particles exhibited a similar size and morphology, they were able to be successfully separated from a mixed suspension of SiO_2 and TiO_2. Moreover, by applying a reasonable bias voltage to the electric tweezer and customizing the size and shape of the tweezer tip, individual 500, 750, and 1000 nm TiO_2 spheres could be easily trapped from the corresponding TiO_2 suspension. The displacements of atomic force microscope (AFM) cantilevers indicated that the forces to trapped a single particle gradually increased with the diameter of the particles. Additionally, the electric tweezer could precisely manipulate a single particle, and stack a specific structure on the top of the electric tweezer. When the electric tweezer was combined with an optical microscope, it could successfully transfer a 5 μm SiO_2 sphere to a HeLa cell. Precisely trapping and manipulating micron and submicron particles is the foundation for fabricating microdevices to achieve specific functions, and it also show great potential for use in biological applications.

© 2025 Published by Elsevier B.V. on behalf of Chinese Chemical Society and Institute of Materia Medica, Chinese Academy of Medical Sciences.

Manipulating micro/nanoscale metal, ceramic, biological particles and droplets in trace liquids (<100 nL) is always a challenge in nanoscience [1–4]. Until now, a variety of non-invasive methods, such as applying an external optical fields, acoustic fields, magnetic fields, and electric fields have been precisely designed to manipulate the movement of nanoparticles, achieving the trapping/assembling/releasing of the nanoparticles, which shows significant potential in nanomedicine, biology, and microfluidics [5–8]. As early as 1986, Ashkin *et al.* have achieved three-dimensional trapping of dielectric microspheres using a single laser beam, declaring the birth of optical tweezer technology, resulting in the awarding of the Nobel Prize [9,10]. Through using the laser gradient force effects, it achieved the manipulation of nanoparticles within non-contact and high precision [11–14]. However, optical tweezers usually required high-power lasers, which can produce thermal effects that may cause damage to the particles and failure of the liquid [15–17]. To address this issue, other related techniques, such as magnetic tweezers, and electric tweezers, have been successfully developed, realizing the controllable operation of magnetic and conductive nanoparticles [18–21]. However, achieving individual separation of non-magnetic and dielectric particles becomes quite difficult [22,23]. Furthermore, it is even more challenging to achieve this in trace liquids and high-viscosity liquids [24,25].

* Corresponding authors.
E-mail addresses: lqzhang@ysu.edu.cn (L. Zhang), jhuang@ysu.edu.cn (J. Huang), ydliu@ysu.edu.cn (Y. Liu).

https://doi.org/10.1016/j.cclet.2024.110655
1001-8417/© 2025 Published by Elsevier B.V. on behalf of Chinese Chemical Society and Institute of Materia Medica, Chinese Academy of Medical Sciences.

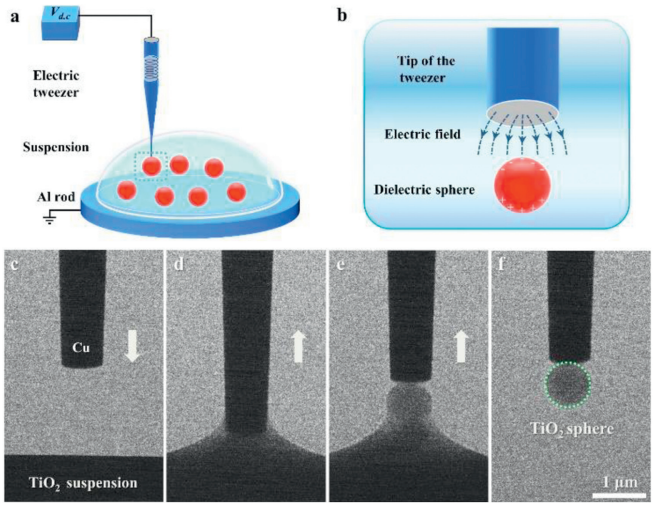


Fig. 1. Electric tweezer submicron sphere extraction process. (a) Schematics of the electric tweezer setup. The electric tweezer was equipped with a force measuring device. The suspension was placed on Al rod, in which dielectric particles could be distributed. (b) Schematic diagram of the sphere extraction process. The dielectric sphere was polarized under the electric field at the tip of the electric tweezer, and then was attracted to the tip of the tweezer by the electrostatic force. (c-f) A single TiO_2 spheres was extracted inside the ETEM by utilizing the electric tweezer. The white arrow indicated the direction of motion of the electric tweezer. The light green dashed circle highlighted the extracted TiO_2 sphere.

In this work, an electric tweezer was designed based on transmission electron microscope and scanning tunneling microscopy (TEM-STM), which manipulated and selectively trapped submicron spheres in suspension by controlling the electric field at the tip of the Cu nanorod. Combined with AFM probe, we successfully measured the force that needed to be overcome to capture 500, 750 and 1000 nm TiO_2 spheres from TiO_2 suspension. Utilizing this technique, 750 nm TiO_2 spheres were successfully trapped from 750 nm and 1000 nm TiO_2 binary suspension. Due to the dielectric constants of various materials to respond to different electric field strengths, TiO_2 particles with the same particle size and similar morphology could be trapped from the mixed suspensions of TiO_2 and SiO_2. Additionally, a SiO_2 sphere was successfully trapped and transferred to the surface of the HeLa cell. Therefore, the trapping and sorting of microscopic particles could be used in nanoscience, engineering, and biomedicine.

The extraction process was conducted inside a Cs-corrected FEI Titan ETEM and equipped with a PicoFemto TEM-STM holder at high temporal and spatial resolutions (Fig. 1a). Firstly, a TiO_2 suspension was placed on one end of the STM probe, and then the half Cu grid with a nano Cu rod was glued to the other end of the STM probe [26,27]. After applying voltage, the Cu rod played as a simple electric tweezer (Fig. 1b). The suspension of high-vacuum silicone pump oil mixed with submicron particles, with high-viscosity and low vapor pressure, can remain stable in the high-vacuum chamber of TEM, thus allowing the visualization of the *in-situ* extraction process of submicron particles in the suspension. The motion of particles in suspension is related to the strength and direction of the electric field. The particles in the suspension become polarized under the action of the electric field, and the polarized particles generate an electrostatic force in the direction of the electric field. At this time, the particles in the suspension will be attracted to the top of the electric tweezer [28]. To assess the feasibility of the electric tweezer, the tip of the Cu rod was immersed in the TiO_2 suspension, then an external electric field was applied.

As shown in Figs. 1c-f, the TiO_2 spheres in the suspension were rapidly polarized and moved toward the electric tweezer under the action of an external electric field (Movie S1 in Supporting information). The electric tweezer side slowly retreated *via* the backward movement of the piezoelectric tube, and the polarized TiO_2 spheres were adhered to the tip of the electric tweezer. According to the distribution of the probe-plate electric field, the electric field was mainly concentrated on the tip of the electric tweezer, where the polarized TiO_2 sphere was subjected to the maximum electrostatic force. When the electric tweezer and suspension were disconnected, a TiO_2 sphere with the same diameter as the tip of the electric tweezer was successfully extracted.

Electric field strength and distribution played key roles in the extraction of individual spherical particles [29,30]. Dielectric particles were arranged along the electric field distribution with an external voltage, and the spherical particles needed to overcome viscous resistance to move in high-viscosity liquids, so there was a critical voltage for extracting individual particles. As shown in Fig. S1 (Supporting information), after the suspension and the electric tweezer connected, a meniscus-shaped interface formed, facilitating the visibility of sphere movement at the interface under different bias voltages. When a 10 V voltage was applied to the electric tweezer, TiO_2 spheres were observed to appear in the thin liquid column area. Due to the limitation of time resolution, the response time to the electric field cannot be detected. As the applied voltage was increased, an increasing number of TiO_2 spheres aggregated at the tip of the electric tweezer. When the voltage reached 50 V, a large number of TiO_2 spheres had already accumulated at the tip of the electric tweezer. Underneath the thick suspension, numerous TiO_2 spheres were stacked, which were difficult to distinguish. However, TiO_2 spheres gathered at the tip of the electric tweezer and the number of spheres increased significantly between 20 V and 30 V. So, we successfully extracted a single TiO_2 sphere at 25 V (Fig. S2 in Supporting information). When the voltage was increased to 50 V, several TiO_2 spheres were extracted on both the top and sides of the electric tweezer (Fig. S3 in Supporting information).

The extraction process described above was used to trap single dielectric particles in a consistent manner. The diameter and shape of the electric tweezer and the electric field strength play a crucial role in the precise extraction of individual dielectric particles. As shown in Fig. S4 (Supporting information), when the diameter of the electric tweezer was larger than the diameter of the spheres to be extracted, after applying a voltage, two spheres appeared at the tip of the electric tweezer. By pulling out the electric tweezer, the two spheres could be accurately extracted. The combined diameter of the two spheres was approximately equal to the diameter of the electric tweezer. The shape of the electric tweezer remarkably affected the distribution of the electric field. As shown in Fig. S5 (Supporting information), three TiO_2 spheres were vertically adsorbed on the conical surface of the electric tweezer tip, aligned along the direction of the electric field under the external bias. After stretching continued, the three TiO_2 spheres were successfully extracted. When the applied voltage exceeded far beyond the critical voltage, the extraction of individual particles became unattainable. As shown in Fig. S6 (Supporting information), a voltage of 75 V was applied, it could be observed that a large number of TiO_2 spheres gathered around the Cu rod due to the higher local electric field strength. After being pulled out, plenty of TiO_2 spheres were extracted on the electric tweezer in a botryoidal form. Therefore, by reasonably designing the diameter and shape of the electric tweezer tip, and applying a suitable voltage, single submicron spheres could be extracted in a controlled manner in the suspension of high viscosity and trace.

Electric tweezers are an advanced technology that utilizes an external electric field to capture submicron particles in suspension. They offered significant advantages in trapping submicron spheres in tandem with TEM for enhanced resolution, and provide the ad-

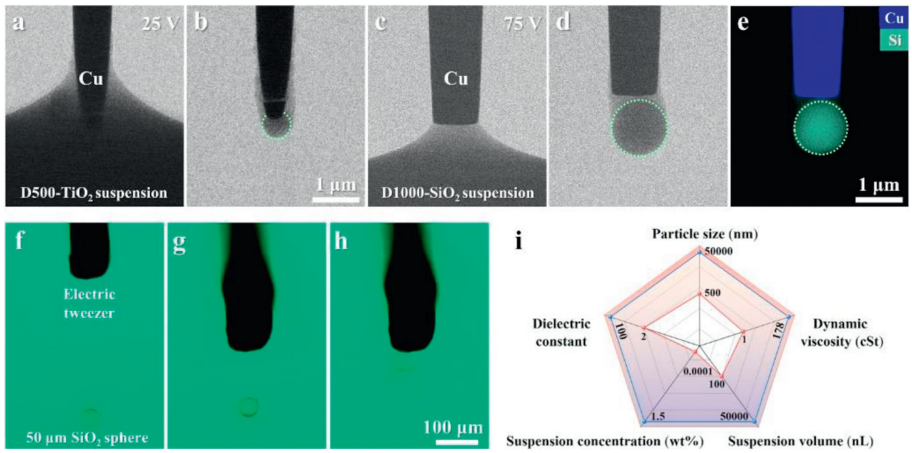


Fig. 2. Electric tweezer extraction process under various conditions. (a, b) The electric tweezer successfully trapped a 500 nm TiO_2 sphere from D500-TiO_2 suspension at 25 V. (c, d) The electric tweezer successfully trapped a SiO_2 sphere from an SiO_2 suspension at 75 V. (e) EDS mapping proved the SiO_2 sphere was adsorbed on the Cu tip. (f-h) A single SiO_2 sphere with a diameter of 50 μm was successful extracted from the suspension at a single particle concentration. (i) Radar chart showing the scope of application of electric tweezers.

justable step size of movement that electric tweezers provide. As shown in Figs. 2a and b, TiO_2 spheres with a diameter of 500 nm were successfully extracted by electric tweezers from D500-TiO_2 (where X = 500 is the diameter of the TiO_2 sphere) suspension at a voltage of 25 V (Movie S2 in Supporting information). The suspension was conducted on an Al rod with a diameter of 0.3 mm and the suspension volume was about 100 nL (Fig. S7b in Supporting information). For the captured particles, the microspheres with a dielectric constant in the range of 2–100 could be captured by adjusting the applied voltage. By increasing the applied bias, the electric tweezer could capture microspheres with lower dielectric properties. Under a voltage of 75 V, the electric tweezers successfully captured the SiO_2 spheres (Figs. 2c-e and Movie S3 in Supporting information). Before reaching the critical voltage, the SiO_2 sphere was adsorbed on the tip of the electric tweezer, but it could not be successfully extracted (Fig. S8 in Supporting information). The SiO_2 spheres which dispersed in the suspension, was in a diameter of approximately 1 μm, exhibited a relatively uniform, monodisperse spherical shape. Energy dispersive X-ray spectrometry (EDS) mapping confirmed the elemental uniformity of the particles (Fig. S9 in Supporting information). The application of electric tweezers is not limited to use with TEM, but also can be in conjunction with optical microscope to capture larger particles (Fig. S10 in Supporting information). In 50 μL of suspension, there were a few scattered SiO_2 spheres, so the particle concentration of the suspension was determined to be 0.0001 wt%. Under an external electric field (Figs. 2f-h), the electric tweezers successfully captured a 50 μm SiO_2 sphere (Movie S4 in Supporting information). The dispersant of the suspension needs to be a non-polar liquid, which is why SiO_2 spheres cannot be captured in a water medium (Fig. S11 in Supporting information). The operating condition of the electric tweezers ranged from atmospheric environment to high vacuum environment, so the viscosity of the dispersing liquid used to disperse micro particles ranged from 1 cSt to 178 cSt. The scope of application of the electric tweezers is summarized in Fig. 2i. The electric tweezers could effectively capture particles ranging from 500 nm to 50 μm. The required suspension volume ranged from a minimum of 100 nL to 50 μL, and the particle concentration distributed in the suspension ranged from a single particle (0.0001 wt%) to 1.5 wt%. By adjusting the applied voltage, dielectric particles with dielectric constants ranging from 2 to 100 could be effectively captured.

For the trapping individual particles, an intermediate voltage of 50 V was chosen to systematically analyze the process of extracting individual particles from suspensions containing TiO_2 spheres with different diameters. Firstly, three different sizes of TiO_2 spheres were synthesized through a sol-gel process as mentioned in materials and synthesis (Supporting information) using HDA as the structure guide agent, and the ratio of H_2O and HDA was adjusted [31]. Scanning electron microscope images show the morphology and diameter evolution from 500 nm to 1000 nm of TiO_2 spheres (Fig. S12 in Supporting information). The TiO_2 spheres were labelled as DX-TiO_2. All the D500-TiO_2, D750-TiO_2 and D1000-TiO_2 spheres had similar smooth surfaces with few craters. There is no obvious aggregation of TiO_2 spheres, and most of them are present as monodisperse spheres. The dimeter of the smallest TiO_2 spheres is approximately 500 nm, which is not conducive for TEM to investigate the interior structure of the samples. For this purpose, all the samples were ultra-microtomed into 80 nm thick sections. TEM images of D500-TiO_2 further reveal monodisperse and regular sphere distribution with a few broken edges, which are attributed to the high hardness of the samples (Fig. S13 in Supporting information). As shown in Fig. S13, D500-TiO_2 spheres possess a homogeneous wormhole-like microstructure, and D750-TiO_2 and D1000-TiO_2 spheres have a similar structure. The corresponding electron diffraction pattern confirmed the amorphous nature of the TiO_2. High angel annular dark field-scanning transmission electron microscopy and corresponding EDS mapping images showed that the Ti and O elements were evenly distributed in the TiO_2, supporting the homogeneous structure formation. According to the above results, it appeared that the only difference among the three samples was in particle sizes. Therefore, the three kinds of TiO_2 spheres with different diameters and high-vacuum silicone pump oil were respectively configured into suspensions for the extraction process.

Firstly, three suspensions of D500-TiO_2, D750-TiO_2, and D1000-TiO_2 were placed on the top of the Al rods. As shown in Fig. S14 (Supporting information), the suspension formed an ellipsoidal shape droplet with a consistent height of approximately 82 μm and a base diameter of 0.3 mm. Then, Cu nanorods were welded onto the conductive AFM cantilever (with a spring constant of 0.4 N/m) to fabricate a force-measuring electric tweezer as shown in Fig. S7 (Supporting information) [32]. The process of extracting TiO_2 particles with different diameters was recorded in real-time. When the suspension was connected with the electric tweezer, it was manipulated slightly backward to form a thin meniscus region between the electric tweezer and the suspension. This can ensure that the side of the Cu rod had minimal liquid, allowing the electric field to concentrate on the cross-section of the electric tweezer tip in liq-

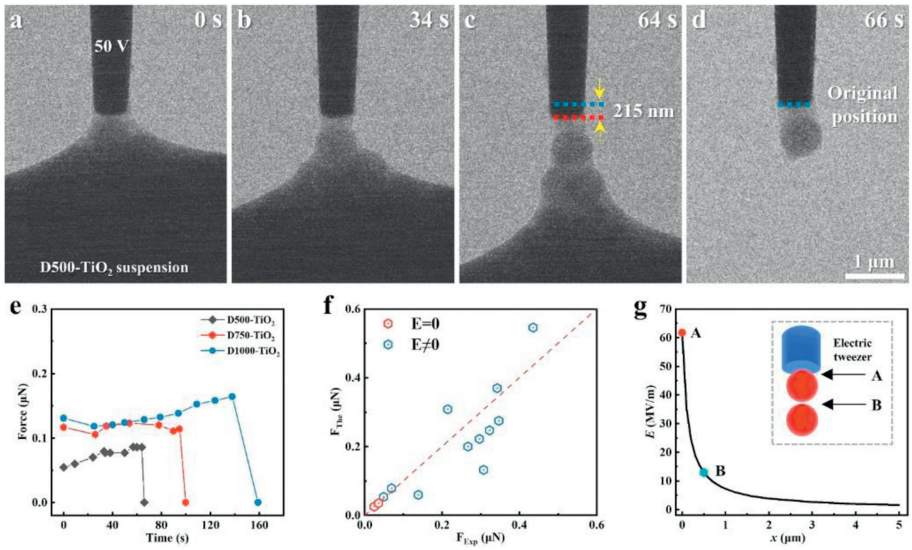


Fig. 3. Mechanical measurement and analysis of electric tweezer extraction process. (a-d) D500-TiO_2 single sphere was extracted. (d) The blue dashed line marked the initial position of the AFM cantilever. (c) The red dashed line marked the position of the AFM cantilever when the electric tweezer extracted a single TiO_2, and the displacement was recorded. (e) Comparison of the force fluctuations during the extraction of D500-TiO_2, D750-TiO_2 and D1000-TiO_2. (f) Comparison of theoretical calculation and experimental measurement. The *x*-axis represented the force measured in the experiment, and the *y*-axis denoted the sum of the calculated capillary and electrostatic forces including $E = 0$ (red plots) and $E \neq 0$ (blue plots). (g) The electric field strength distribution on the tip of electric tweezer. The *x*-axis represented the distance from the electric tweezer tip. The *y*-axis represented the electric field strength.

uid. After the voltage was applied, the spheres in the suspension were more likely to accumulate at the tip of the electric tweezer, so the single sphere could be extracted by controlling the diameter of the Cu rod. In this way, three individual spheres of different sizes have been successfully extracted from three TiO_2 suspensions, respectively. At the same time, the force between the adjacent particles can be calculated based on Hooke's law by recording the displacement of the AFM cantilever in this process.

For D500-TiO_2, when the suspension slowly retreated, it was visible that three separate spheres adsorbed and stacked in the vicinity of the electric tweezer tip due to the external potential (Figs. 3a-d and Movie S5 in Supporting information). The electric field at the electric tweezer tip was modulated by controlling the thickness of the suspension. The adjacent spheres were in complete contact, and the distance between them was barely visible. At this point, the electrostatic force between the sphere and electric tweezer tip reached its maximum value. As the suspension continuously receded, the distance between the adjacent spheres increased, forming a liquid bridge in between. As the liquid bridge breaks up, a single D500-TiO_2 sphere was extracted. As shown in Fig. 3c, the displacement *x* of AFM was 215 nm, which provided the real-time force record of the single sphere extraction. Then, the process of single particle extraction from suspension composed of D750-TiO_2 and D1000-TiO_2 spheres was systematically studied, respectively. As shown in Figs. S15a-e (Supporting information), the extraction process of D750-TiO_2 was similar to that of D500-TiO_2. Upon the withdrawal of suspension, the distance between the top sphere and the neighboring bottom spheres slightly increased, resulting in the decrease of electrostatic force between the spheres and eventually they separated. The displacement of the AFM cantilever was recorded as $x = 285$ nm. As depicted in Figs. S15f-j (Supporting information), when the electric field was applied, it could be seen that D1000-TiO_2 spheres arranged beneath the suspension, after which the D1000-TiO_2 suspension was slowly receded, and a single D1000-TiO_2 sphere was captured. The displacement of the AFM cantilever could be accurately measured, and the displacement *x* was 410 nm. During the extraction processes, the positions of the AFM cantilever were recorded in real-time, reflecting the force variation trend of the entire system in extracting TiO_2 spheres (Fig. 3e). The maximum tensile forces measured by AFM cantilever are summarized in Table S1 (Supporting information). During the measurement of tensile force, the electron beam irradiations do indeed affect the inherent viscosity properties of the suspension. The aforementioned measurement process was conducted under a low-dose electron beam irradiation (5 e nm^{-2} s^{-1}). At a higher electron beam dose (50 e nm^{-2} s^{-1}), as the electric tweezer was pulled out, a gel-like liquid bridge was formed, with a large number of TiO_2 spheres distributed (Fig. S16 in Supporting information).

For the entire electric tweezer system, the major forces to be overcome during the extraction of spheres are the capillary force F_c and electrostatic force F_e. Regarding the capillary force, the surface tension coefficient of the suspension was measured to be $\gamma = 33$ mN/m by Du Nouy ring method [33]. The capillary force F_c between the adjacent particles upon liquid bridge breakup consists of a surface tension force at the contact line, $\gamma \pi l$, and Laplace force due to the pressure difference ($2\gamma/l$) across the liquid bridge surface, $-\gamma \pi l/2$ [34,35]. Thus we have

$$F_c = \gamma \pi l / 2 \tag{1}$$

Here l is the diameter of the liquid bridge neck (Fig. S17 in Supporting information). Without applying any bias voltage, the capillary force between the adjacent particles upon liquid bridge breakup was measured with the force-measuring electric tweezer [36]. The electric tweezer tip was first immersed in the suspension, and then the liquid side was slowly retracted. At the instant that the Cu rod and the suspension were about to separate, the displacement of the AFM cantilever and the diameter of the liquid meniscus were recorded as illustrated in Fig. S17. The surface tension calculated by AFM displacements was 0.025 μN and 0.036 μN respectively, which is consistent with the value calculated by Eq. 1 (Fig. 3f). This also demonstrated that the liquid retained its inherent viscosity properties.

While the formula of capillary force is validated, we still need to calculate the electrostatic force between spheres to explain the trap of a single particle. Based on a pin-plate geometry assumption, the electric field intensity at the axis between the tweezer

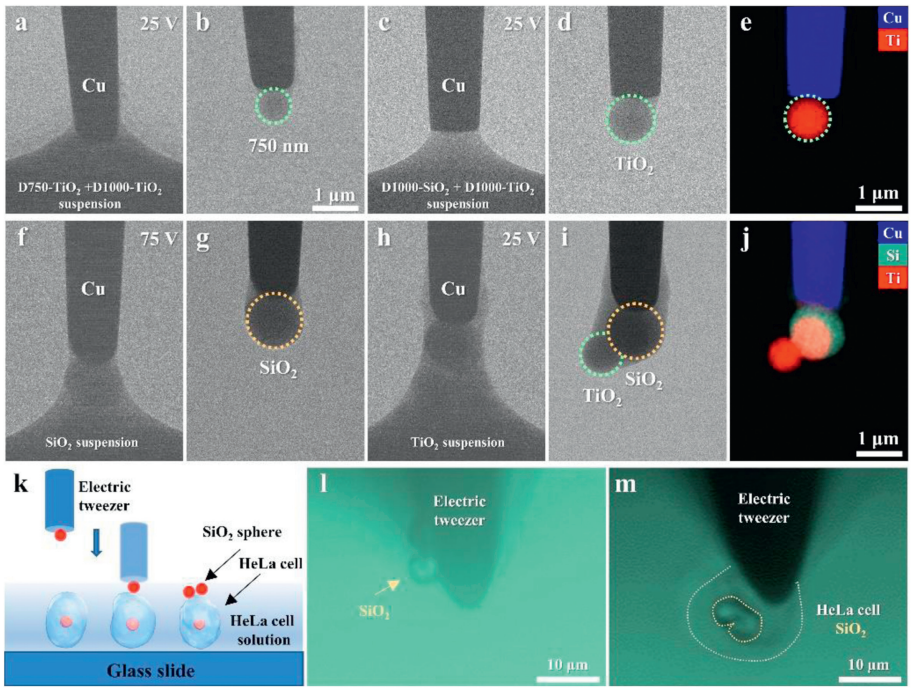


Fig. 4. The application of electric tweezer. (a, b) The electric tweezer separated a 750 nm TiO_2 sphere from D750-TiO_2 and D1000-TiO_2 binary suspensions. (c-e) The electric tweezer trapped a TiO_2 sphere from D1000-TiO_2 and D1000-SiO_2 binary suspensions, proved by EDS mapping. (f-j) Through repeated extraction processes, the SiO_2 and TiO_2 sphere were extracted respectively, and a specific structure was stacked on the tip of the electric tweezer. (k) Schematic representation of the transfer process of microparticles to the HeLa cell surface. (l) Optical microscope image showing SiO_2 spheres adsorbed on the electric tweezer. (m) SiO_2 spheres were successfully transferred to the surface of a HeLa cell.

tip and the plate is expressed as [37]:

$$E = \frac{2V}{(R+2x_0)\ln\left(2d/R+1\right)} \tag{2}$$

where x_0 is the distance from the tip of the tweezer to the bottom of the first sphere, R is the radius of curvature of the tip, d is the distance between the tweezer tip and the plate, V is the applied voltage, as shown in Fig. S18a (Supporting information). All the involved geometry parameters can be measured by the optical or electron microscope images. Fig. 3g shows that the electric field intensity decays rapidly with increasing x_0.

Then, the electrostatic force between the adjacent particles in an electric field can be calculated based on the theoretical formula proposed by Lekner *et al.* [38]:

$$F_e = \frac{1}{18}\pi^5\epsilon E^2\frac{r_p^3}{s}\left(\frac{1}{2}\ln\frac{4r_p}{s}+0.5772\right)^{-2} \tag{3}$$

where s is the distance between two adjacent spheres and assumed to be 0.5 nm here, ϵ is the dielectric constant of the surrounding liquid, as depicted in Fig. S18b (Supplementary information). The attracting force between two adjacent particles can be theoretically calculated as $F_{The} = F_c + F_e$. Fig. 3f compares the theoretically obtained F_{The} with the force measured in the experiment F_{Exp}. The data points were distributed around the red dotted line, which proved that the theoretical calculation results were in good agreement with the experimental measurements. When extracting a single TiO_2 sphere, the electric field distribution at the electric tweezer tip is depicted by Fig. 3g. The electric field strength at the electric tweezer tip (position A) is 4.77 times larger than that between the first and second particles (position B). Given that the capillary forces between the two locations are similar, so the attractive force at position A is greater in comparison according to Eq. 3. Although the electrostatic force between the second particle and the particles below is smaller than the electrostatic force at position B due to the smaller E, the diameter of the liquid bridge below it is much larger, resulting in a much larger capillary force. Therefore, the attraction between the first and second particles is smaller than the total attraction between the second particle and the two particles below it. That is, the attraction between the first and second particles is the smallest and the easiest to break. Therefore, the electric tweezer successfully trapped a single particle.

The self-developed electric tweezer traps submicron particles by exploiting the response of dielectric particles to electric fields. Through theoretical calculations, the forces required to capture 500, 750 and 1000 nm TiO_2 spheres gradually increased. In the binary suspensions of D750-TiO_2 and D1000-TiO_2, the electric tweezer was more inclined to capture D750-TiO_2 particles (Figs. 4a and b, Movie S6 in Supporting information). To test the versatility of the electric tweezer, numerous attempts were made to capture submicron particles in binary suspension systems, which was homogeneously mixed by thorough physical oscillation and ultrasonic dispersion (Fig. S19 in Supporting information). SiO_2 and TiO_2 spheres have similar morphologies and particle sizes, so are extremely difficult to separate. Considering that the dielectric constant of SiO_2 spheres is approximately 2, significantly lower than that of TiO_2 spheres. Therefore, the particles can be extracted from the suspension by exploiting the differences in the dielectric constants of the two particles. According to the above results, there were noticeable voltage differences in extracting TiO_2 and SiO_2 spheres. At 25 V, for the binary suspension system composed of TiO_2 spheres and SiO_2 spheres, the electric tweezer could extract a single sphere (Figs. 4c and d, Movie S7 in Supporting information). Despite the similar morphology and particle size of TiO_2 and SiO_2 spheres, the extracted sphere could be identified as TiO_2 by EDS mapping (Fig. 4e). As the voltage increased to 50 V, as shown in Figs. S20a-d (Supporting information), the number of TiO_2 particles extracted at the top of the electric tweezers significantly increased. EDS confirmed that no SiO_2 spheres were present among the extracted TiO_2 particles, with some silicone oil residue on the sur-

face. When the voltage was further raised to 100 V, a large number of submicron spheres were adsorbed at the top of the electric tweezers, as shown in Fig. S20e (Supporting information). EDS results confirmed that both TiO_2 and SiO_2 spheres were adsorbed at the top of the electric tweezers, as illustrated in Figs. S20f-h (Supporting information).

The electric tweezer not only can extract a single sphere, but also construct a single sphere chain structure through repeated extraction. Firstly, a single sphere was extracted at the tip of the electric tweezer. Then, the electric tweezer was inserted into the suspension, and the extraction process was repeated, as shown in Fig. S21 (Supporting information). Thereafter, another sphere was extracted and adhered to that was previously extracted. The extraction process can be repeated multiple times, and a short chain with three spheres can also be obtained (Fig. S22 in Supporting information).

By repeating the capture process, heterogeneous structures can also be stacked on the electric tweezer tip. As shown in Figs. 4f-i, the electric tweezer was first immersed in the SiO_2 suspension and the SiO_2 sphere was successfully captured at a voltage of 75 V. Then the electric tweezer was immersed into the TiO_2 suspension and the TiO_2 spheres were adsorbed on the SiO_2 sphere at 25 V, thus successfully building a heterogeneous structure of a SiO_2 sphere and TiO_2 spheres (Movie S8 in Supporting information). The corresponding EDS mapping also proved that two TiO_2 spheres were adsorbed on the SiO_2 sphere (Fig. 4j).

In addition, the electric tweezers can also capture one single micron particle and transfer it to the surface of a HeLa cell. The capture and transfer process are shown in Fig. 4k. First, the electric tweezer was immersed in a suspension dispersed with 5 μm SiO_2 spheres, and one side of the suspension was grounded (Fig. S10). Under the action of an external electric field, the SiO_2 spheres were successfully captured on the electric tweezer tip (Fig. 4l). Then, the electric tweezer adsorbed with SiO_2 spheres was immersed in an aqueous solution dispersed with HeLa cells, one side of the aqueous solution was grounded, and a voltage of 0.5 V was applied to the electric tweezer (Fig. S23 in Supporting information). Since the cell membrane was negatively charged, the HeLa cells were adsorbed on the electric tweezer, and the SiO_2 spheres were transferred to the surface of the HeLa cells through gentle vibration (Fig. 4m).

In this study, a nanoscale electric tweezer has been designed by using *in-situ* ETEM. This unique electric tweezer could effectively trap particles of different polarity such as SiO_2 or TiO_2 spheres with diameters ranging from 500 nm to 50,000 nm, distributed in liquids with a single particle or concentrations up to 1.5 wt%. The viscosities of liquid ranged from 1 cSt to 178 cSt. The influences of the particle diameter on electrostatic forces and surface tension during the trapping of individual particles were accurately assessed through measuring the displacement of the AFM cantilever. Under the action of an external electric field, the dielectric particles were polarized and moved in a controllable manner in the suspension. The electric field at the tip of the tweezer was concentrated, and the electrostatic force between the particles at tip was sufficient to overcome the surface tension of the suspension and the electrostatic force between the particles, thereby capturing the particles. On this basis, this unique electric tweezer could separate SiO_2 and TiO_2 spheres in the mixed suspension. In comparison to other techniques, it provides highly visual operation during the particle trapping process with greater accuracy and the ability to trap particles with a wide range of diameters and dielectric constants. In addition, the electric tweezers demonstrated excellent applicability in optical microscopy and successfully transferred dielectric particles to the HeLa cell surface. The electric tweezers we designed are efficient and precise, showing considerable application potential in micro-nanostructure design and biomedicine.

Declaration of competing interest

The authors declare that they have no known competing financial interests or personal relationships that could have appeared to influence the work reported in this paper.

CRediT authorship contribution statement

Hui Li: Writing – review & editing. **Zhenjie Zhao:** Visualization. **Bingqiang Ji:** Formal analysis. **Jun Ma:** Methodology. **Xuwu Zhang:** Methodology. **Jingzhao Chen:** Methodology. **Zhangran Ye:** Methodology. **Zuankai Wang:** Visualization, Supervision. **Liqiang Zhang:** Supervision. **Jianyu Huang:** Visualization, Validation, Supervision. **Yingdan Liu:** Visualization, Validation, Supervision.

Acknowledgment

This work was financially supported by the National Natural Science Foundation of China (Nos. 52372293, 52471018), the S&T Program of Hebei (Nos. B2023203037, B2024203054), the Science Research Project of Hebei Education Department (No. JZX2024022), Central Guidance Fund for Local Science and Technology Development Project (No. 246Z1101G).

Supplementary materials

Supplementary material associated with this article can be found, in the online version, at doi:10.1016/j.cclet.2024.110655.

References

[1] C. Baur, A. Bugacov, B.E. Koel, et al., Nanotechnology 9 (1998) 360.
[2] B. Polyakov, S. Vlassov, L.M. Dorogin, et al., Beilstein J. Nanotechnol. 5 (2014) 133–140.
[3] C.D. Onal, O. Ozcan, M. Sitti, Automated 2-D Nanoparticle Manipulation With an Atomic Force Microscope, IEEE ICRA, Kobe, 2009, pp. 1814–1819.
[4] Y. Jin, W. Xu, H. Zhang, et al., Proc. Natl. Acad. Sci. U. S. A. 119 (2022) e2105459119.
[5] O.V. Salata, J. Nanobiotechnol. 2 (2004) 3.
[6] S. Hettiarachchi, H. Cha, L. Ouyang, et al., Lab Chip 23 (2023) 982–1010.
[7] T. Chen, C. Huang, Y. Wang, J. Wu, Chin. Chem. Lett. 33 (2022) 1180–1192.
[8] C.G. Yang, R.Y. Pan, Z.R. Xu, Chin. Chem. Lett. 26 (2015) 1450–1454.
[9] A. Ashkin, J.M. Dziedzic, J.E. Bjorkholm, S. Chu, Opt. Lett. 11 (1986) 288–290.
[10] A. Ashkin, J.M. Dziedzic, T. Yamane, Nature 330 (1987) 769–771.
[11] G.B. Ashis, C. Sagar, K.G. Satyandra, L. Wolfgang, J. Biomed. Opt. 16 (2011) 051302.
[12] S. Ghosh, A. Ghosh, Nat. Commun. 10 (2019) 4191.
[13] D.G. Grier, Nature 424 (2003) 810–816.
[14] D. Gao, W. Ding, M. Nieto-Vesperinas, et al., Light Sci. Appl. 6 (2017) e17039.
[15] K.B. Crozier, Light Sci. Appl. 8 (2019) 35.
[16] Q. Jiang, B. Rogez, J.B. Claude, et al., ACS Photonics 6 (2019) 1763–1773.
[17] M.B. Rasmussen, L.B. Oddershede, H. Siegumfeldt, Appl. Environ. Microbiol. 74 (2008) 2441–2446.
[18] K. Dholakia, B.W. Drinkwater, M. Ritsch-Marte, Nat. Rev. Phys. 2 (2020) 480–491.
[19] S. Yang, J. Rufo, R. Zhong, et al., Nat. Rev. Phys. 18 (2023) 2441–2458.
[20] F.J. Alenghat, B. Fabry, K.Y. Tsai, et al., Biochem. Biophys. Res. Commun. 277 (2000) 93–99.
[21] D.L. Fan, F.Q. Zhu, R.C. Cammarata, C.L. Chien, Nano Today 6 (2011) 339–354.
[22] J. Chen, D. Liu, J. Qiu, et al., IEEE Photon. J. 14 (2022) 1–4.
[23] H. Başağaoğlu, S. Succi, D. Wyrick, J. Blount, Sci. Rep. 8 (2018) 8583.
[24] G.D. Chen, F. Fachin, M. Fernandez-Suarez, et al., Small 7 (2011) 1061–1067.
[25] X. Mu, W. Zheng, J. Sun, et al., Small 9 (2013) 9–21.
[26] J.Y. Huang, L. Zhong, C.M. Wang, et al., Science 330 (2010) 1515–1520.
[27] X. Huang, X. Guo, Y. Ding, et al., Chin. Chem. Lett. 32 (2021) 598–603.
[28] B.W. Kwaadgras, M. Verdult, M. Dijkstra, R. van Roij, J. Chem. Phys. 135 (2011) 134105.
[29] Y. Nakajima, T. Matsuyama, J. Electrostat. 55 (2002) 203–221.
[30] A. Sihvola, J. Nanomater. 2007 (2007) 45090.
[31] D. Chen, L. Cao, F. Huang, et al., J. Am. Chem. Soc. 132 (2010) 4438–4444.
[32] D. Erts, A. Lõhmus, R. Lõhmus, H. Olin, Appl. Phys. A 72 (2001) S71–S74.
[33] R. Macy, J. Chem. Educ. 12 (1935) 573.
[34] P. Lambert, A. Chau, A. Delchambre, S. Régnier, Langmuir 24 (2008) 3157–3163.
[35] O.H. Pakarinen, A.S. Foster, M. Paajanen, et al., Model Simul. Mat. Sci. Eng. 13 (2005) 1175.
[36] Y. Tong, Z. Wu, B. Zhou, et al., Chin. Chem. Lett. 35 (2024) 109062.
[37] O.V. Kim, P.F. Dunn, Aerosol. Sci. Technol. 44 (2010) 292–301.
[38] J. Lekner, J. Appl. Phys. 114 (2013) 224902.